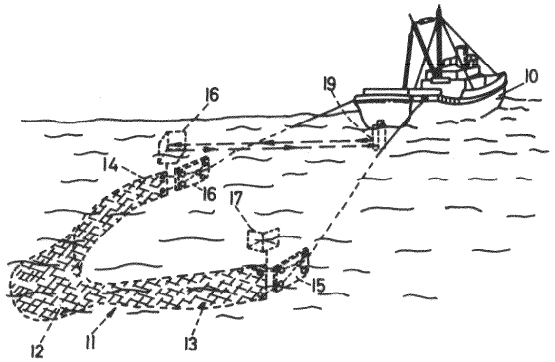

FIG. 11d-1. Diagrammatic representation of a system for underwater echo signaling for checking the position of fishing nets.

sheer boards, but still below the water surface, there can be seen fastened to the net the triple reflectors, 17 and 18, suitable for sound reflection.

Triple reflectors or mirrors, as is well known in the art, have three reflecting, substantially square planes, each perpendicular to the other two as the three sides adjacent to a corner of a cube. A ray of light or a beam of sound impinging upon the inner surface of one of these three planes is reflected in its direction of incidence so that one receives at the point of transmission always a total reflection from the triple mirror no matter what inclination it takes. Such total or complete reflection is very effective and relatively low transmitter energy will result in strong echo signals which surpass in intensity by far the interferences introduced by the water surface and make possible clear and definite observation.

The vessel, 10, carries an ultrasonic transmitter, 19, which beams an ultrasonic signal toward triple reflector, 17 or 18. When the ultrasonic beam strikes one of the reflectors, the beam is reflected in the direction of incidence, i.e. toward the transmitter, 19. Thus the location of the net, the position of the

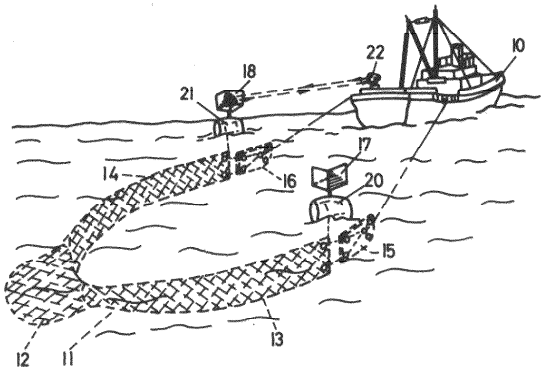

FIG. 11d-2. Diagrammatic representation of a system for light pulse reflector signaling for checking the position of fishing nets.

sheer boards with respect to each other, and therefrom the quantity of catch, can be determined.

Somewhat similar results to those with sound having ultrasonic frequency under water can be obtained by employing a light beam and optical triple mirrors above the surface of the water as depicted in Fig. 11d-2. Here the triple mirrors, 17′ and 18′, are secured to floats or buoys, 20 and 21, extending to the water surface at points of the net located above the sheer boards. A searchlight, 22, mounted on the deck of the fishing vessel, sends a beam of pulse light toward the mirrors, and light incident on either one of the mirrors will be reflected in the direction of incidence in the same manner as sound under water.

In triple reflectors for sound having ultrasonic frequency the three planes forming the reflector are preferably constructed to render good total reflection against water. Such construction consists, for instance, of air filled, thin walled sheets of metal or other material having a considerably different wave resistance from that of water; for example, brass or steel.

2. AIR IMPULSE SOUND

a. *Theoretical Considerations on the Characteristic Sound Spectrum of Capacitor Discharges and Their Experimental Verification* [202]

Spontaneous electric discharges of capacitors are generally accompanied by an intense detonation-like noise, which can be imagined to originate as follows: The air which is permeated by the electric charge is subjected to a sudden temperature rise and thus develops a certain overpressure against the surrounding air. Consequently, there is a tendency for pressure equalization, and the compressed zone starts to expand in all directions. In the zones of slight overpressure the pressure wave proceeds in accordance with the differential equation of the sound field. Here a simple example may illustrate what slight temperature changes are sufficient to cause considerable sonar effects.

It is assumed that a spherical air volume of 1 cm diameter is subjected to a temperature rise of 10 °C in such a short time that no measurable volume expansion could occur during the heating-up interval. The pressure increase will then amount to 3.3×10^4 μbar. If we take the laws of sound propagation for granted, then an observer at 1 meter distance would measure a pressure change of 165 μbar. This impulse as such is comparatively short; however, it is prolonged by the many reverberations from the walls of the room and thus gains considerable intensity. If one recalls that normally the human ear is accustomed to sound pressure values in the region of 1 μbar, then he will see that the value of 165 μbar represents a considerable noise level.

The calculations made in [202] result in a time dependency of the sound pressure of

$$p = P_0 e^{-\alpha t}$$

with

$$\alpha = \frac{1}{T} = \frac{3c}{r}\sqrt{1 + \left(\frac{c}{\omega r}\right)^2}$$

where

p = overpressure in μbar
P_0 = overpressure at $t = 0$
t = time
T = time constant
c = speed of sound
r = radius of a sphere in free atmosphere
$\omega = 2\pi f$
f = sound frequency

If one applies to this formula the rules of Fourier's analysis a relation results for the Fourier coefficients $A(\omega)$ which are a measure of the amplitudes of the partial tones.

$$A(\omega) = \frac{1}{\pi} \frac{1}{\sqrt{\omega^2 + \left(\frac{3c}{r}\right)^2 \cdot \left(\frac{c}{\omega r}\right)^2 + \left(\frac{3c}{r}\right)^2}}$$

The sound spectrum increases with the frequency and, as it progresses further, the gradient becomes less steep and finally comes to a halt at a maximum. Figure I2a-1 shows graphs of sound spectra of pressure equalization phenomena calculated for various spherical starting volumes. The pressure amplitude is indicated per cycle and related to the surface of the starting volume per sound pressure unit. The numbers beside the curves indicate the radius of the sphere.

The maximum will be found at that frequency where the wave length λ is 3.5-fold the radius of the sphere. There is one particularly noteworthy fact: At the higher frequencies the spectra of all spherical radii enter into the same boundary line.

The deductions applying to the pressure equalization process in free atmosphere can also be modified to suit two further characteristic cases. If the equalization process does not occur over the frequency dependent, sound resistance of a spherical radiator of 0 power but over the frequency independent sound resistance of an exponential funnel, then also the decaying constant becomes frequency independent. If it is assumed that the cross sectional area of the connected funnel is equal to the surface of the initial sphere then

$$\alpha = \frac{1}{T} = \frac{3c}{r}$$

If this value is inserted in the equation for $A(\omega)$, the result turns out to be characteristic spectrum of an e-function. The process is likewise illustrated in Fig. 12a-1 for various sphere diameters or initial volumes. Within the range $\alpha > \omega$ the sound pressure amplitude per cycle is constant. In the course of further progress, when $\alpha < \omega$ there occurs the same drop-off as formerly with $1/\omega$. The difference between the two curves is due to the spherical radiator's drop-off in sound resistance toward the low frequenceis. The value of α is apparently determined by the relation of the initial volume to the cross

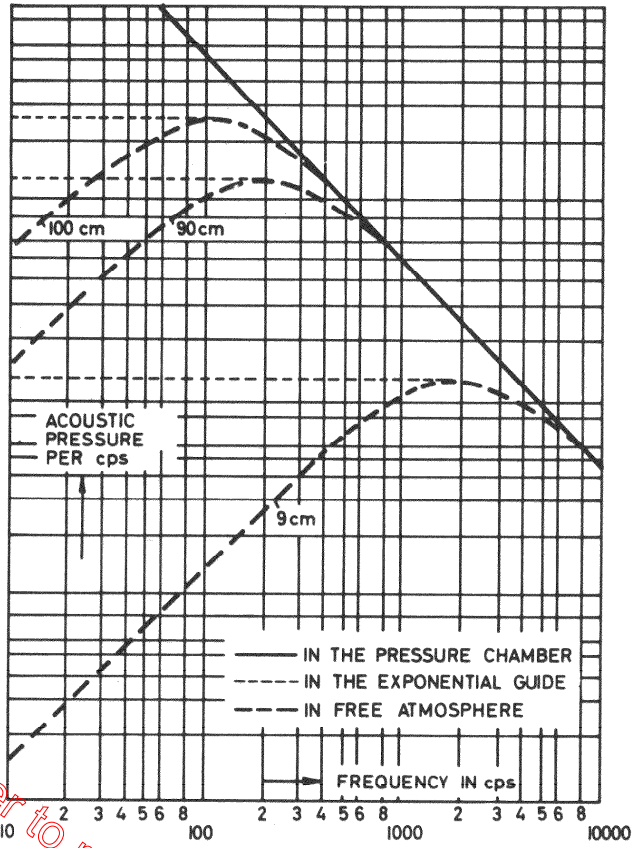

FIG. I2a-1. Graph of the calculated acoustic spectra in pressure equalization phenomena for various spherical starting volumes. The acoustic pressure amplitude is stated per cps per acoustic pressure unit in relation to the starting volume surface. The numbers at the curves state the radius of the sphere.

sectional opening area of the funnel. The radius of the assumed sphere is found by experimental results.

Another characteristic case is found when the capacitor discharge occurs within an enclosed space the relative size of which is small in comparison with the smallest wavelength. In such circumstances a pressure equalization will no longer be possible. In this case $\alpha = 0$. The amplitude of the partial tones, drops monotonously with increasing frequency (see Fig. 12a-1, drawn-out line). This fact is thoroughly comprehensible since at the moment of the capacitor discharge there occurs a pressure jump in the vessel which is of extremely long duration compared to the time scale applied here.

Figure I2a-2 shows the phase angles of partial tones during a pressure equalization in relation to the frequency for a spherical volume of $r = 5$ cm.

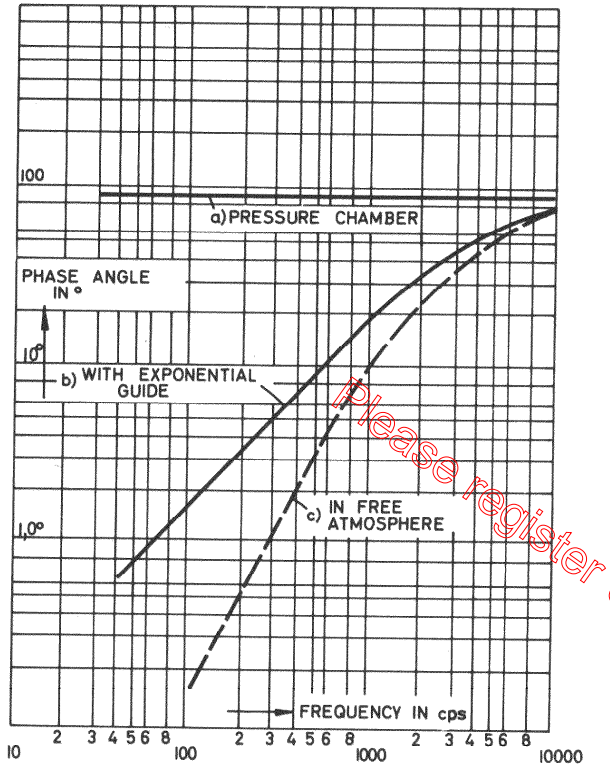

FIG. I2a-2. Phase angle of the partial tones during a pressure equalization phenomenon in relation to the frequency for a spherical volume of 5 cm radius. a–pressure chamber; b–with exponential horn; c–in free atmosphere.

Curve a relates to the pressure vessel, curve b to the exponential funnel and c to free atmosphere.

Of great importance also are the phase relations among individual partial tones since measuring results can be influenced by them, particularly during performance of the octave sifting analysis in the sound absorbing chamber. In the pressure chamber experiment all partial tones have the same initial phase of 90°. In the case of pressure equalization in free air the phase shifts from nearly 0° at the low frequencies up to 90° at high frequencies. A similar curve form results from a frequency independent time constant.

Figure I2a-3 shows measuring results obtained in the sound absorbing chamber at 30 cm distance between sound emitter and microphone for various sonar pulses. The peak sound pressure value per octave is indicated above the point of frequency concentration of the corresponding octave in the region from 37.5 cps to 12,000 cps. The sonar pulses originated from capacitor discharges at different electric energy levels and from the report of a Flobert pistol. The measuring results do not lend themselves to comparison with the theoretical values in Fig. I2a-1 since they relate to sound pressure per octave

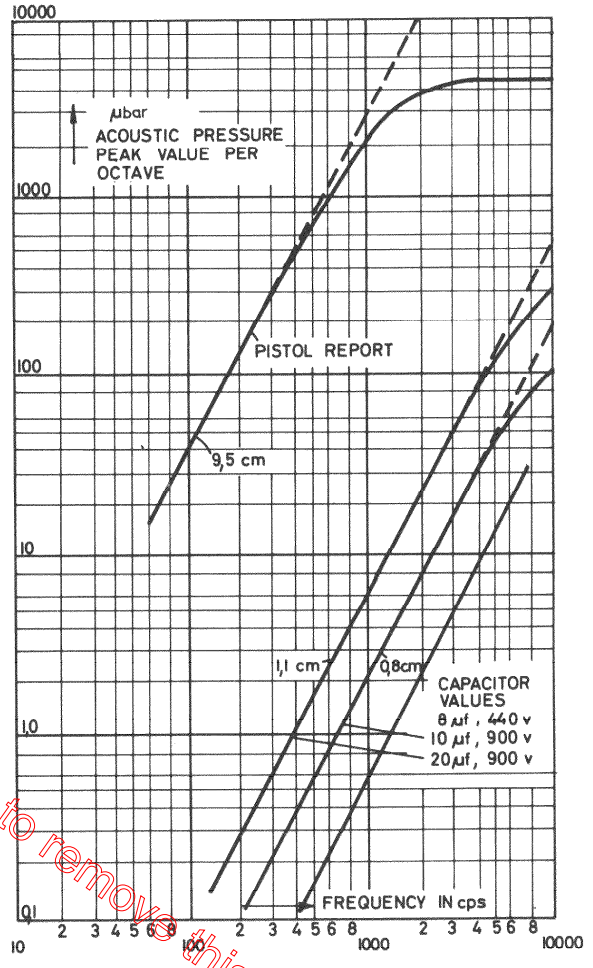

FIG. I2a-3. Measurements in a nonresonant room at 30 cm distance. Acoustic pressure peak value per octave in relation to the frequency for different reports. The centimeter indications at the curves indicate the size of the marginal radius determined from the spectral characteristic (at the curves 9.5 cm and 1.1 cm the references to the constant octaves have been omitted; hence, the much more erratic values.

at 30 cm distance, while the theoretically computed values relate to sound pressure per cps at the unit of sound pressure. In order to make possible a comparison of the measured curves with the computed curves of Fig. I2a-1, at least in their progress, they have been related to the sound pressure value per cps by dividing the measured sound pressure values by the bandwidth of the corresponding octave. This simple dividing procedure is applicable in this case since the phase shifting within one octave is only slight. In the octave

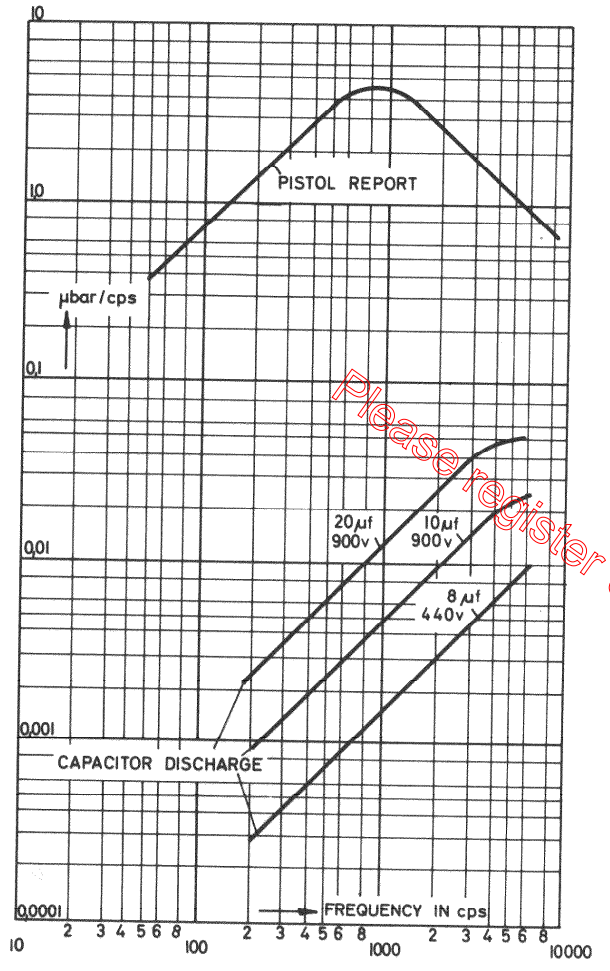

FIG. I2a-4. Graphs of the acoustic spectrum per cps for various reports related to 30 cm measuring distance calculated from the acoustic pressure values per octave measured in the nonresonant room.

embracing the maximum of the partial tone spectrum there is merely a phase shift of approximately 20°.

In all other cases only values of roughly 5° occur. The phase shiftings within the octave filter as such, particularly at the flanks, do not reflect on the curve shape since, as already mentioned, the error is identical in all octaves. The corrected curves are shown in Fig. I2a-4 and their shape is identical to that of the theoretically computed curves. Consequently, for the start of the sound wave we must assume a certain radius of the sphere. The measurements further indicate that the size of the sphere's radius depends on the energy released. Apparently the pressure wave first expands from its center of origin

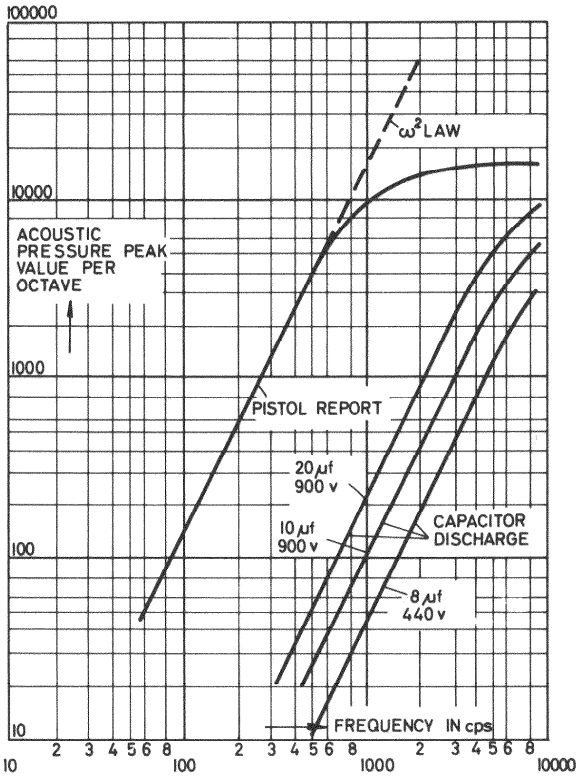

FIG. I2a-5. Measurements in a nonresonant room. Acoustic pressure peak value per octave related to the surface of the sphere, the marginal radius of which has been calculated from the spectral characteristic.

at supersonic speed until a radius is reached where the overpressure has dropped down to such a value that the linear acoustic laws begin to apply. The marked appearance of the separation point can be explained by assuming that at an adiabatic change of conditions between pressure and radius there exists the relation

$$\frac{P_1}{P_2} = c\left(\frac{r_1}{r_2}\right)^{4.2}$$

i.e. at a linear change of the radius the pressure change will proceed by the 4.2 power.

The increase of the radial boundary proportional to the energy released finally points to the conclusion that the same pressure must always prevail on the surface of the marginal sphere. In order to check this, the pressure values measured at a certain distance were reduced to the spherical radius determined from the spectrum. As can be seen from Fig. I2a-5, all curves tend to enter into an upper marginal value of approximately 15,500 μbar per

octave, while in the ascending part the distance between the curves corresponds to the square of radial relations, as could be expected because of the changing radiation resistance. Thus the same starting pressure on the surface of the sphere with the critical radius has been proved for all cases in question.

The considerations relating to the pressure equalizing phenomena with regard to the pistol shot report can no doubt also be applied to other explosion phenomena, provided that the assumptions accepted in the derivation with regard to the steep gradient of the pressure jump will also be valid. But after all, it is in the very nature of explosion phenomena that a very steep pressure increase occurs. For instance, a sound analysis of the recorded acoustic spectrum of an internal combustion engine without exhaust showed the same mathematical interrelationship as in the above-discussed laws. The two-stroke engine seems to meet the theoretical conditions best because of its short exhaust stroke. It may also be assumed that the muzzle blast of heavier firearms will proceed according to identical physical laws.

To summarize, one can say that it is safe to assume that the overpressure of an acoustic sphere in free atmosphere is equalized over the sound resistance of the sphere's surface. The Fourier analysis of the equalizing process leads to a continuous sound spectrum; the partial tone intensity per cps at the lower frequency range increases similarly to the radiation resistance of a radiator of 0 power, that is, in proportion to the frequency up to a maximum occurring at that frequency where the wavelength of the partial tone has reached the 3.5-fold radius of the air sphere. Then follows a drop off of the partial tone intensity which is inversely proportional to the frequency. On double logarithmic coordinate paper the spectral curve becomes a bell-shaped curve, ascending symmetrically to the maximum. The size of the sphere's radius determining the shape of the spectral curve depends on the total energy which has been set free. However, independent of the total energy, the common value for the pressure jump on the sphere's surface is approximately 150,000 μbar. This seems to be the limit where the linear acoustic laws begin to apply, while up to this point the pressure equalization process proceeds at supersonic speed. From the pressure jump as such one can, if the equalization process is taken into account, calculate the sound energy, whereby the calculated results can be verified experimentally. The sound spectra of capacitor discharges can be used for determination of the frequency curves of microphones in free atmosphere. The measuring accuracy so far achieved is 1 db. If the capacitor discharge noise is released in the muzzle of an exponential funnel one can determine the radiation characteristic of the latter. Finally, the report of a pistol shot—which often is used for room acoustic measurements—has been for determining the frequency dependent characteristic of acoustic energy.

b. *Air Shock Waves in Traffic Safety*

This additional use was discovered by Bradfield. His ultrasonic blind guiding device utilizes a capacitor discharge of 1 to 1.5 μsec duration occurring 3 or 4 times per second at the focal point of a parabolic mirror. The transmitted "white" ultrasonic spectrum is reflected from an object and received by a crystal microphone located in a second hollow mirror. Devices of the same principle are useful in traffic safety control and are also used for automatic garage door openers.

The crack sound that emanates from an air spark is not low in its efficiency as might be assumed, since it is a strictly adiabatic sound radiation. The capacitor energy is converted in the spark plasma mostly into heat and only a small portion is lost by light radiation within the visible and invisible range. Thus the major portion of the energy remains as thermal energy and exerts itself, in accordance with the basic laws of adiabatic expansion, as mechanical and thus acoustic energy radiation. Only the facts that very high frequencies are immediately absorbed in air and other gases, due to nonideal behavior, and that a high percentage of the spark sound lies in the extremely high ultrasonic range, lead to the condition that a short distance away from the spark only low frequencies—and these with only low efficiencies in accordance with their modest Fourier participation—can be found in the "white" frequency band of the spark sound. The effect of this condition can be eliminated to a certain degree by utilizing an oscillatory circuit, the half-waves of which produce a sparkover each time so that, in accordance with the Fourier analysis, a main frequency is obtained that is twice the current cycle frequency and the sparkover frequency. This procedure, however, does not change the fact that every sparkover again produces high primary frequency portions which are subjected to the same lamentable high momentary absorption in the near vicinity of the spark.

Ultrasound generation by means of spark discharges belongs to the field of thermal ultrasonic generators. Exactly speaking, it is not proper to refer to ultrasonics when this method of sound generation is meant, because in connection with ultrasonics there is normally understood a definite frequency, whereas the property of the spark sound is to radiate a white spectrum and thus no frequency. Sound and "crack" have the same relationship as ultrasound and "shock wave sound" when the latter term is introduced with a corresponding meaning. With spark discharges it is possible to generate high shock sound peak outputs which could never be produced with conventional means, for instance, several hundred kilowatts peak outputs. In the following section some applications of shock sound and its generation are illustrated.

c. *Applications of Air Shock Waves*

In order to conclude the discussion about emission of shock sound in gases or atmospheric air, the construction of a radiator for crack sound waves in air will be illustrated. One of its uses is to scare birds.

A simple arrangement is shown in Fig. I2c-1. An electric capacitor, 1, is periodically charged and, after being charged it discharges itself through the electrodes, 2, with a cracking sound spark. The electrodes, 2, are so located that the issuing shock sound radiation can be projected in the desired direction as a narrow beam; for instance, at the focal point of a reflector, 3. For radiation in all directions, an electrode system as depicted in Fig. I2c-2 is suitable. The electric spark, fed from capacitor, 1, jumps the gap between the

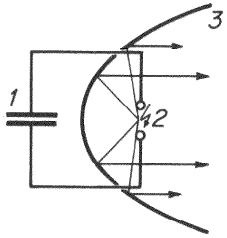

FIG. I2c-1. Electrical capacitor discharge by means of a sound spark gap for production of parallel directed, impulse sound radiation.

contact metal faces, 2, which are fastened to suitably curved metal sheets, 3, so that the shock sound originating from the spark travels in all radial directions as indicated by the arrows, 4. Since the contacts, 2, produce the electric spark in atmospheric air, they are subjected to strong oxidation. The most suitable electrodes for resisting oxidation are made of sintered metal, such as tungsten-silver.

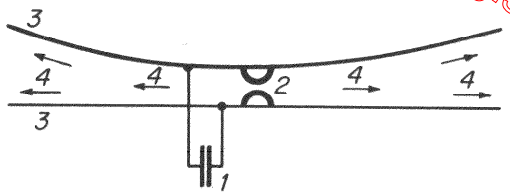

FIG. I2c-2. Electrodes ystem for all-around radially emerging disturbance sound creation.

For physiological crack sound production it is known by experience that 1 to 50 crack sparks per second will suffice. The charge of the capacitor must be at least 1/10 watt-sec. The electrode spacing is dependent on the maximum current value of the spark. The maximum current value in turn depends on the inductance lying in the discharge circuit or formed by it. The frequency components above 100 kc have such a limited radiation range in air that their production is uneconomical; the more so, since the share of higher frequencies becomes ineffective due to absorption. Thus, an inductance, 3, is inserted in the discharge circuit of capacitor 1 including electrodes 2 as indicated in Fig. I2c-3a. The value of this inductance must be such that, as illustrated in Fig. I2c-3b, the first half-wave with its duration t coincides with a half-wave of the desired emission frequency.

Example:

Desired electrical charge for one spark:	$\frac{1}{2}CU^2 = 1/4$ watt-sec
Capacitor value:	10,000 pf
Charging voltage:	7,000 volts
Inductance for critical damping:	100 kc 1/4000 h = 250 μh
Charge of capacitor in amp-sec	$Q = CU = 7 \times 10^{-5}$ amp-sec
Spark resistance of the first half-wave:	$R_F = k \times l/Q = 16/7$ ohm for $k = 0.8 \times 10^{-3}$
Sparking distance for 7 kv:	assumed as $l = 0.2$ cm

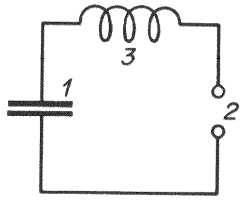

FIG. I2c-3a. Spark circuit with capacitor and line inductance.

The ohmic resistance of inductance 3, Fig. I2c-3a, must, for prevention of substantial losses, be lower than the spark resistance, which is 16/7 ohm in the present example. By applying a high frequency litz-wire coil it is possible to obtain with small outlay a coil resistance of 0.5 ohm, which is low enough not to weaken the crack sound noticeably, but to assist in releasing the full sound energy within the range of the effective frequency.

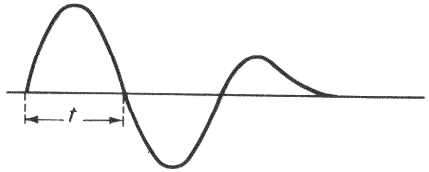

FIG. I2c-3b. Oscillogram of the discharge wave damped by the spark.

Charging of the capacitor, as shown by the example, requires only little electrical energy. For 50 sparks/sec the electrical energy would be 50 watts and including the nonavoidable charging losses this would require a power supply of 100 watts, whereas with a spark frequency of one/sec, which is usually still sufficient, the consumption is only 1 to 2 watts. If it is desirable to charge capacitor 1 from the ac power line, as illustrated in Fig. I2c-4 a high leakage transformer, 5, is interposed in the circuit. Its leakage inductance, 6, is by proper measures adjusted so that during each voltage half-wave there takes place only one capacitor charge up to the breakdown voltage of the spark gap. Transformers originally designed for neon tube illumination of the lowest commercial ratings are well suited for the purpose under consideration. For shielding high frequency oscillation from the secondary of such transformers, a small capacitor, 2, is connected in parallel to this winding whereby

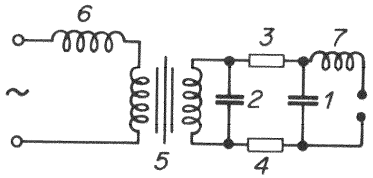

FIG. I2c-4. Equivalent circuit diagram for charging of a capacitor from the ac power line by means of a leakage transformer.

charging of capacitor 1 is effected through the charging resistance, 3 and 4. The voltage pulses at capacitor 1 thus become ineffective at the transformer so that completely radio-interference-free operation is assured.

3. Shock Sound by Underwater Capacitor Discharges

a. *Spark Breakdown in Liquids*

Electrically conductive liquids such as salt solutions in water and alcohol can be used for enforcing a spark discharge by means of sufficiently great and quickly increased voltage differences between two metal electrodes. The electric potential gradients determine the breakdown voltage, which is a characteristic constant for the substance in question, just as, for instance, are conductivity and the dielectric constant.

For experimental purposes solutions of salts and acids were used mainly with low salt concentrations of 5%, where the conductivity as far as distilled water is concerned would change from 1 to 1000 and more. One or several capacitors in parallel were charged to high voltage potentials and the discharge was fed through a 2 mm copper conductor, which was interrupted at two places by spark gaps. Seen from the capacitor, the first spark gap was an air gap between brass spheres of 2 cm diameter with variable distance and the second spark gap was between brass spheres of 1.4 cm or 1 cm diameter at a certain distance. With this arrangement Heydweiller [217] found breakdown voltages of 200-800 kv/cm.

Similar to the direct sparkover in liquid mediums is the process with the electrolytic interrupter, which will be described because of the similarity of the phenomena involved. Two forms of the electrolytic interrupter must be distinguished, the Wehnelt interrupter and the Simon interrupter.

The Wehnelt interrupter [218] consists of a glass vessel filled with dilute sulphuric acid in which two electrodes are submerged. The positive electrode is a thin platinum wire, which protrudes only a few millimeters from an insulator. The negative electrode is formed by a lead plate. The interruption occurs when, at the small surface of the platinum wire, owing to the heavy current, a bubble of nonconductive vapor forms, caused by evaporation as well as electrolytic decomposition. The sudden interruption generates an overvoltage, which causes a sparkover in the gas bubble and therefore explodes the latter. The nonexplosive part of the gas bubble is blasted away by the explosion. The liquid then again contacts the wire and the voltage rise can start over again.

The Simon interrupter [219] operates in a similar manner. This interrupter has two large lead electrodes in sulphuric acid. They are separated from each other by a very narrow diaphragm. The current must pass through this diaphragm and thus creates at the place of greatest current density a vapor bubble which causes interruption.

By means of electrolytic interrupters up to several thousand interruptions per second can be attained. Every single interruption or disconnection is so sudden and so complete that a parallel capacitor becomes unnecessary with these interrupters. Also the electrolytic interrupters permit a certain control:

With the Wehnelt interrupter, for instance, the depth to which the platinum wire is submerged can be varied; with the Simon interrupter, control is effected by increasing or decreasing the diaphragm, e.g. by lowering a china cone more or less deeply into the diaphragm and thus partly closing the latter. Figure 13a-1 is a schematic diagram of the Wehnelt and Simon interrupters.

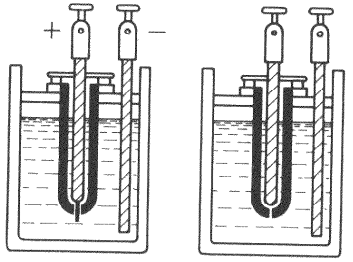

FIG. I3a-1. Schematic diagram of the Wehnelt and Simon interrupters.

L. R. Padberg [60] gives an incomplete compilation of a number of measurements made in cases where resonators were excited by fluid sparks. Further literature in this connection is given under [220, 229, and 101].

TABLE I3a-1

ACOUSTICAL AND MECHANICAL EFFICIENCY OF LIQUID SPARK GAPS (REPRODUCED FROM [53])

$C(\mu f)$	U(kv)	$\frac{1}{2}CU^2$ (mw-sec)	R	$L(\mu h)$	Weight (gm)	Throw height (cm)	Mech. work (cm-gm)	Mech. work (mw-sec)	Efficiency (%)
0.012	18.3	2000	—	0.2	2	130	260	26	1.3
0.012	18.3	2000	—	0.2	1.4	170	240	24	1.2
0.067	12.2	5000	—	0.2	5	100	500	50	1
0.067	12.2	5000	—	0.2	2	200	400	40	0.8
0.067	12.2	5000	—	0.2	2	250[a]	500	50	1
0.07	12.2	5200	—	0.2	20	25	500	50	0.96
0.07	12.2	5200	—	0.2	5	150	750	75	1.44
0.07	12.2	5200	—	0.2	2	200	400	40	0.8
0.07	12.2	5200	2.5	0.2	2	100	200	20	0.4
0.07	12.2	5200	—	3	5	100	500	50	0.95
0.07	12.2	5200	—	82	5	50	250	25	0.47

[a]Height to ceiling of room. Every one of above values is an average of 3–5 single measurements which scatter by ± 20%.

Investigations concerning the mechanical efficiency of liquid sparks were made by Früngel [53] on small weights thrown up by liquid sparks (see Table I3a-1). The results show efficiencies on the order of 1%, because it is impossible to establish mechanical-acoustic adaptation between weight and

This simple initial ignition results in a very considerable oscillation excitation within the plasma.

The arrangement shown is also suitable for all capacitor discharge circuits with relatively low resistive loads. It works with potassium or sodium instead of mercury as fill-gas. Mercury, however, is the least temperature dependent. For an operating inverse voltage of 5000 volts at 5000 amp nonoscillating or oscillating impulse current load with oil cooling, the device needs only chamber sizes of about 2 liters capacity.

At high average loads, e.g. at impulse sequences of 100 kw-sec/sec (100 kw), under adverse conditions, several kilowatts in loss heat are produced within the switch tube. Therefore, it is advisable to provide for operation under oil as illustrated in Fig. B4-6. The oil in turn is cooled by rib coolers with water. In order to keep the vapor pressure, and thereby the ignition conditions, in the tube constant, the temperature must be maintained at a constant level (e.g., 40°C). Temperature and pressure, however, must not surpass a certain limit. Otherwise the breakthrough voltage may become dangerously low. During the starting period, and a short time thereafter, temporary heating of the tube may be necessary for the above reasons. After the operating temperature has been reached, the heating may be changed to cooling in order to carry off the continuously generated operating heat. If the switching device is cooled by circulating water, which in industrial plants generally has a temperature of 25–40°C, too low a starting temperature is practically excluded beforehand.

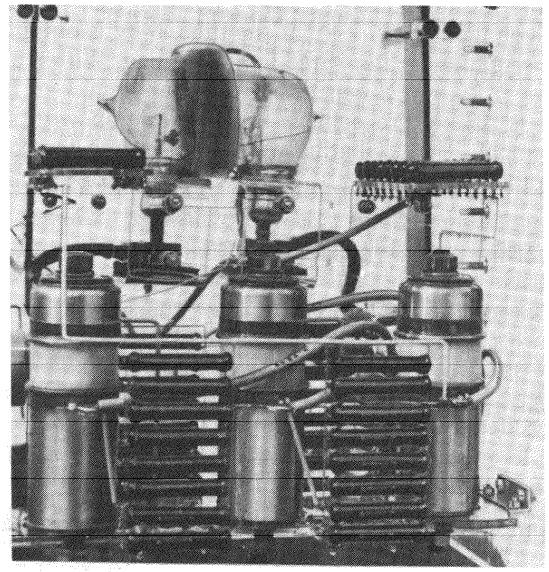

FIG. B4-6. Internal arrangement of an inductron switching. The cascade impulse capacitors can be seen subdivided at the left, middle, and right of the illustration, above the inductron tube with the ignition coil.

Because of their long life, inductively ignited diodes are referred to as "duratrons."

5. Fixed Spark Gaps

a. *Measuring Spark Gaps with Two Electrodes*

Spark gaps appear to be the earliest switching means for capacitor discharges. The techniques for measuring high capacitor discharge potentials and high ac voltages are dependent upon them. They form the basis of standard high-potential measuring methods. It is well known that in a sphere spark gap the breakdown or sparking distance depends on the diameter of the spheres and the air pressure. There are tabulations available from several sources in which measured potentials and corresponding sphere diameters are listed (see Tables B5a-1 and B5a-2). The measuring potentials are referred to normal barometric air pressures and have to be converted to values of acutally prevailing pressures. Throughout wide limits, within the validity range of Paschen's law, the breakdown voltage varies in linear direct proportion to the air pressure. The simplest form of switching mechanism is the connection of a capacitor with a load through an interposed fixed spark gap. When the capacitor is charged to a potential that surpasses the breakdown potential of the spark gap (which can be adjusted to within 3% or even more accurately), the sparkover occurs. The spark in the gap now has a spark resistance that was first calculated by Toepler. The resistance of the spark R_F according to Toepler, which is sufficiently accurate for practical purposes, is

$$R_F = \frac{k \times l}{Q}$$

wherein $k_{\text{air}} = 0.8 \times 10^{-3}$ (see Chapter M), l is the length of the spark in centimeters and Q is the number of ampere-seconds transmitted through the spark. A spark which discharges a 1 μf capacitor charged to 30 kv through a spark gap of about 1 cm length would have a resistance of

$$R_F = \frac{0.8 \times 10^{-3} \times 1}{10^{-6} \times 3 \times 10^{4}} = 8/300 \text{ ohm} \approx 27 \text{ milliohms}$$

From this example it becomes apparent that the spark resistance is negligibly low in comparison with the usual resistances of loads into which capacitors are discharged. The widespread belief that a spark is an undesirable source of high losses is thus not justified. A modification of the solid state or self-igniting spark gap is an arrangement in which one sphere of the gap is made movable with respect to the other sphere. The movable sphere is advanced toward the other by a pneumatic or electromagnetic actuator until breakdown occurs or the electrodes strike each other. In rough use under heavy loads with very high current peaks the spheres may weld together. In order to avoid this it is advisable to provide a small circular recess in the sphere and to fill it, level to the sphere surface, with tungsten so that tungsten will strike against tungsten. Even under current impulses of many thousand

170. Früngel, F. Hochspannungs-Prüfgeräte mit hyperbolischer U-I-Kennlinie. *Elektro-Welt* **4,** (C3), 67-68 (1959).

171. Früngel, F. Vorrichtung zum Messen und Dosieren von Elektrizitätsmengen. German Patent 971,719 (Aug. 30, 1951).

172.* Fischer, H. Simple submicrosecond light source with extreme brightness. *J. Opt. Soc. Am.* **47** (11), 981-984 (1957).

173.* Fischer, H. Funkenkanäle extremer Leistung. *Physik. Verhandl.* **6,** 177 (1955).

174. Freise, W., and Früngel, F. Zur Messung des Verlustwinkels von grossen einseitig geerdeten Kapazitäten. *Elektrotech. Z.* **80** (10), 296-300 (1959).

175.† Zuckermann, W. A., and Awdejenko, A. L. *Zhur. Techk. Fiz.* **7,** 185 (1942.)

176.† Zuckermann, W. A. *Vorträge Akad. Wiss. USSR* **40,** 7 (1943).

177.† Zuckermann, W. A. *Vorträge Akad. Wiss. USSR* **53,** 4 (1946).

178.† Strachowski, G. M., and Zuckermann, W. A. *Izvest. Akad. Nauk. SSSR, Ordel. Tekh. Nauk.* **3,** (1946).

179.† Zuckermann, W. A., and Manakowa, M. A. *Zhur. Tekh. Fiz.* **27,** 391 (1957)

180.† Lukaschw, A. A. *Pribory i tekhn. eksperim.* **4,** 56 (1957).

181.† Sjusin, W. P., Manakowa, M. A., and Zuckermann, W. A. *Pribory i tekhn. eksperim.* **1,** 85 (1958).

182.‡ Dummer, G. W. A. "Fixed Capacitors." Pitman, London (1956).

183.‡ Dummer, G. W. A. "Fixed Capacitors" pp. 149-152. Pitman, London (1956).

184.‡ von Tersch, L. W. and Swago, A. W. "Recurrent Electrical Transients," pp. 18-27, 320-332. Prentice-Hall, Englewood Cliffs, New Jersey (1953).

185.‡ Lebacqz, J. V. and White, H. J. The rotary spark gap. *In* "Pulse Generators," pp. 275-292. McGraw-Hill, New York (1948).

186.‡ Germeshausen, K. J. The hydrogen thyratron. In "Pulse Generators," pp. 336-344. McGraw-Hill, New York (1948).

187.‡ Dillinger, J. R. General considerations for gap design. In "Pulse Generators," pp. 316-332. McGraw-Hill, New York (1948).

188.* Chace, W. G., and Moore, H. K. "Exploding Wires," pp. 197. Plenum Press, New York (1959).

189.‡ Dillinger, J. R. The three-electrode fixed spark gap. In "Pulse Generators," pp. 332-335. McGraw-Hill, New York (1948).

190.† Goldberg, S., and Germeshausen, K. J. On the design and measurement of hydrogen thyratron modulator characteristics. A summary interim report of findings under Signal Corps Development contract DA 36-029 sc 15372 (1953).

191. Früngel, F. Quick-Responsive spark gap device. U.S. Patent 2,886,737 (May, 1959).

192.‡ White, H. J., Gillette, P. R. and Lebacqz, J. V. The pulse-forming network. *In* "Pulse Generators." pp. 201-213. McGraw-Hill, New York (1948).

193.* Hawley, W. G. "Impulse Voltage Testing," pp. 32-34. Chapman & Hall, London (1959).

194.† Hauser, S. M., and Quan, H. Applying the Kerr cell to nanosecond. *Electronics* pp. 57-59 (Aug., 1961).

195.† McFarlane, H. B. Spark gaps for fast high voltage switching. *Electronics* pp 72-73 (July, 1959)

196. Früngel, F. Quenching spark gaps as trigger elements in high speed cinematography. *Proc. 5th Intern. Congr. on High Speed Photography, Washington,* 1960. pp. 469-472. Society of Mot. Pic. and Tel. Eng., New York (1962).

197.* Dessau-Righ. Die elektrischen Wellen. In "Die Telegraphie ohne Draht," p. 177. Vieweg, Braunschweig (1907).

198.* Zenneck, J. Die technischen Löschfunkenstrecken. "Lehrbuch der drahtlosen Telegraphie," pp. 222-226. Springer, Berlin (1925).

199.* Wien, M. Über eine Methode zur Erzeugung schwach gedämpfter elektrischer Schwingungen. *Physik. Z.* **9** (2), 49 (1908).

200.* Boas, H. Löschfunkenstrecken für enge Koppelung. "Jahrbuch der drahtlosen Telegraphie," p. 563 (1912).

201.* Weichart, F. Funkenstrecken: (a) Knall-oder Knarrfunkenstrecken; (b) Löschfunkenstrecken; (c) Funkenstrecken mit rotierenden Elektroden. "Jahrbuch der drahtlosen Telegraphie," pp. 420-422 (1928).

202.† Weber, W. Das Schallspektrum von Knallfunken und Knallpistolen mit einem Beitrag über Anwendungsmöglichkeiten in der elektroakustischen Messtechnik. *Z. Akustik* **4,** 373-391 (Nov., 1939).

203.* McFarlane, W. The sound radiation from a condenser discharge. *Phil. Mag.* [7] **7,** 117 (July, 1934).

204.* Geiger, H. and Scheel, U. K. in "Handbuch der Physik" (H. Geiger and K. Scheel, eds.), Vol. VIII, Chap. 14, p. 635. Springer, Berlin (1926).

205.* Schindelin, W. Beiträge zur Raumakustik. *Ann. Physik* [4] **52,** 129 (1920).

206.* von Békésy, G. Über die mechanische Frequenzanalyse einmaliger Schwingungsvorgänge und die Bestimmung der Frequenzabhängigkeit von Übertragungssystemen und Impedanzen mittels Ausgleichsvorgängen. *Z. Akustik* **3** (5), 217 (1937).

207.† Behnke, A. Über die Speicherung mehrerer durch Flüssigkeitsfunken erzeugter seismischer Impulse auf einem einzigen magnetischen Tonträger. *Z. Geophysik* **26** (1), 24-31 (1960).

208.* Suhr, G. Eine neue Apparatur zur Messung des vertikalen Gradienten der seismischen Wellengeschwendigkeit. Dissertation, University of Hamburg (1956).

209.† Baule, H., and Müller, E. Messung elastischer Eigenschaften von Gesteinen. *In* "Handbuch der Physik" (S. Flügge, ed.), Vol. 47, pp. 180-189 Springer. Berlin (1956/57).

210.* Vogel, C. B. A seismic velocity logging method. *Geophysics* **17,** 3 (1952).

211.* Bradfield, G. Precise measurement of velocity and attenuation using ultrasonic waves. *Nuovo Cimento 7,* Suppl. 2, pp. 162-181 (1950).

212. Früngel, F. System for probing materials by shock wave signals. U.S. Patent 2,946,217 (May, 1955).

213.* Schardin, H. Das Töplersche Schlierenverfahren. *VDI-Forsch.* Ausgabe B, p. 367 (1934).

214.* von Schmidt. O. Über Knallwellenausbreitung in Flüssigkeiten und festen Körpern. *Z. Physik* **39,** 868 (1938); Über Kopfwellen in der Seismik. *Z. Geophysik* **15,** 141 (1939).

215.* Mintrop, L. 100 Jahre physikalische Erdbebenforschung und Sprengseismik. *Naturwissenschaften* **34,** 257, 289 (1947). Über Anwendung des seismischen Verfahrens im Erdölbergbau und ihre wirtschaftlichen und wissenschaftlichen Auswirkungen. *Öl und Kohle* p. 269 (1943).

216.† Müller, E. Eine neue Messmethode zur Bestimmung der Wellengeschwindigkeiten in Gesteinsproben. *Naturwiss. Rundschau* **41** (4), 85 (1954).

217.† Heydweiler, A. Über die dielektrische Festigkeit leitender Flüssigkeiten. *Z. Instrumentenk.* **12,** 377 (1892); *Ann. Physik* [3] **48,** 110 (1893).

218.* Wehnelt, A. *Elektrotech. Z.* **20,** 76 (1899); *Ann. Physik* [3] **68,** 233 (1899).

219.* Simon, H.Th *Ann. Physik* [3] **68,** 860 (1899).

220.* Anderson, V. C. Wide band sound scattering in deep scattering layers. *Scripps Inst. Oceanog. Contribs.* Reference 53-36 (1953).

221.* Burhorn, F., *et al.* Temperature measurements of water stabilized high power arcs. *Z. Physik* **131** (1), 28-40 (Dec. 1951).